05,08

Magneto-optical effects in nanostructures $Bi_xY_{3-x}Fe_5O_{12}$/r-Al_2O_3

© A.V. Telegin, Yu.P. Sukhorukov, I.D. Lobov, S.V. Naumov, Yu.V. Korkh, S.S. Dubinin, K.A. Merencova, M.S. Artemiev, A.P. Nosov

M.N. Mikheev Institute of Metal Physics of Ural Branch of Russian Academy of Sciences, Yekaterinburg, Russia

E-mail: telegin@imp.uran.ru

Received July 17, 2025
Revised July 17, 2025
Accepted July 19, 2025

Ultrathin films of yttrium-iron garnets with bismuth ($Bi_xY_{3-x}Fe_5O_{12}$) on sapphire substrates (r-Al_2O_3) have been synthesized by magnetron sputtering. The spectral dependences of the Faraday effect and the polar Kerr effect in $Bi_xY_{3-x}Fe_5O_{12}$/r-Al_2O_3 thin-film nanostructures are considered. The dispersion of the Verdet constant and the polar Kerr effect for a substrate made of monocrystalline diamagnetic r-Al_2O_3 has been measured. The spectral and field dependences of the Faraday and Kerr rotations of $Bi_xY_{3-x}Fe_5O_{12}$ films have been determined. It is shown that the diamagnetic transparent substrate r-Al_2O_3 makes a weak contribution to the magneto-optical characteristics of thin-film nanostructures. The presence of magnetic inhomogeneities as a result of island growth of $Bi_xY_2Fe_5O_{12}$ films on r-Al_2O_3 is accompanied by a significant decrease in the magnitude of the Faraday and Kerr effects. At the same time, the magnitude of the effects in the $Bi_xY_{3-x}Fe_5O_{12}$ films grown on r-Al_2O_3 still is the same order to that of $BiY_2Fe_5O_{12}$ films on garnet substrates, which opens up prospects for wider use of $Bi_xY_{3-x}Fe_5O_{12}$/r-Al_2O_3 structures either for research purposes or for practice.

Keywords: Faraday effect, Kerr effect, Verdet constant, ferrite garnet, sapphire, magnetic inhomogeneities, thin films.

DOI: 10.61011/PSS.2025.08.62265.197-25

1. Introduction

When creating compact planar devices of magneto- and opto-electronics, it is relevant to develop procedures of synthesis of ultra-thin magnetic films with preservation or improvement of their functional properties. Of particular interest is yttrium iron garnet YIG ($Y_3Fe_5O_{12}$) and its bismuth-substituted form BiYIG ($BiY_2Fe_5O_{12}$), which have high transparency and high magnetooptical (MO) characteristics of the Faraday and Kerr effects in the visible and near-IR spectral ranges at the room temperature [1–5].

The low-dimensional thin-film structure exhibit effects related to the morphology, the thickness and the structure of the film material. For example, when the film thicknesses are reduced to a nanometer scale, their magnetic and magnetooptical properties are largely affected by growth defects as well as interlayer interfaces and structural specific features at a film/substrate boundary. Incompliance of the parameters of crystal lattices of the film and the substrate results in origination of mechanical stresses and, as a result, formation of dislocations and formation magnetically dead and/or magnetically passive layers that deteriorate the structural, magnetic, transport and magnetooptical characteristics of the films [6–8]. Therefore, for the BiYIG films, structurally-similar single crystals of low-magnetic garnets are used as substrates and exemplified by $Gd_3Ga_5O_{12}$ (GGG), $Nd_3Ga_5O_{12}$, $Y_3Al_5O_{12}$ (YAG), etc.) [1]. These substrates are characterized by high dielectric constant, transparency, thermal resistance and low eigenvalues of the magnetooptical effects [9–13]. However, due to high cost these materials are mainly used for scientific purposes and still are not widely applied in a modern industry of production of the thin-film optoelectronic instruments. An alternative option for creating the BiYIG-based magnetooptical structures is to use single-crystal sapphire (r-Al_2O_3). Sapphire is widely applied in modern microelectronics due to its high optical- and radio-transparency, mechanical and temperature strength [14,15]. Besides, it is more technological and commercially available as compared to garnet (GGG, YAG) or nitride (GaN) substrates. All this determines a potential interest to its application for optimizing technologies of creating various devices: Faraday isolators, UHF filters, hybrid photon-spintronic platforms, etc. [2–4]. At the same time, sapphire without a buffer layer is seldom used for synthesis of the yttrium iron garnet due to a high difference of the lattice parameters of the film and the substrate as well as their coefficients of thermal expansion, which result in cracking and discontinuity of the film layer. Therefore, the data on the magnetooptical effects in these structures are scarce, although their study is of particular interest. Besides, as shown in the recent studies [6,7,13,16], in case of the nanoscale thicknesses of the BiYIG layers the optical and magnetooptical parameters of bulk substrates can strongly affect the characteristics of the nanostructures due to proximity of values of a magnetooptical response.

Thus, there are relevant tasks related both to producing the high-quality ultra-thin magnetic BiYIG layers

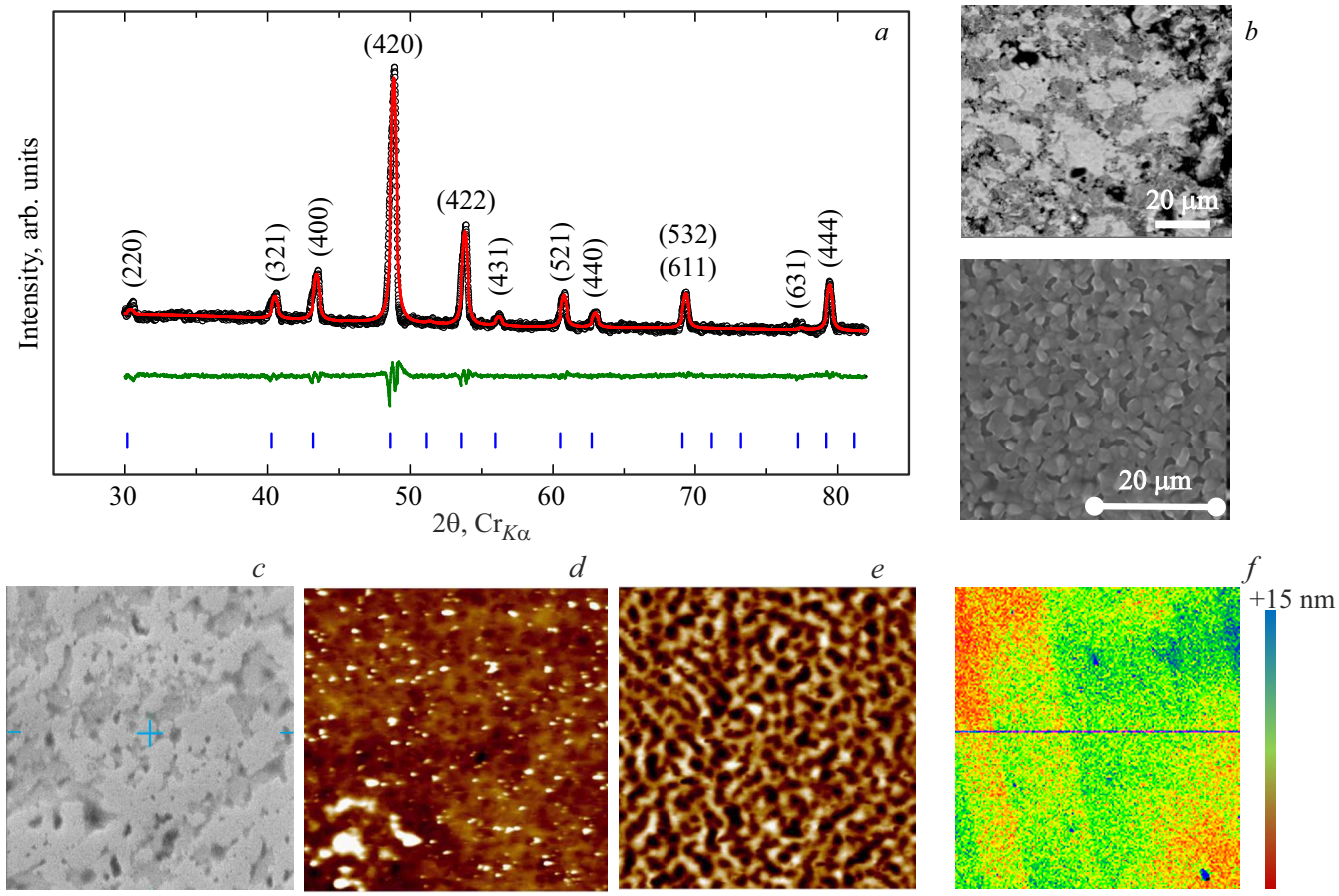

Figure 1. (a) Diffraction patterns in the large angles $\theta - 2\theta$ for the $BiY_2Fe_5O_{12}$ target (CrK_α radiation). The black symbols mark experimental values, the red line marks a calculation and the green line marks a difference between the experiment and the calculation. The vertical blue markers denote positions of Bragg peaks. (b) Morphology of the target surface according to scanning electron microscopy data at various magnifications. The scale markers are provided in the figures. (c) The image of the surface of the BiYIG film of the thickness of 54 nm in secondary electrons, (d) probe microscopy data: topography and (e) data of probe microscopy: the magnetic-force contrast images of the film surface (the size of the scanning area is everywhere $20 \times 20\,\mu m^2$). One can see clear magnetic contrast which is not related to the morphology of the film surface. (f) Data of optical profilometry for the BiYIG film. The scanning area is $200 \times 200\,\mu m^2$. The color contrast reflects slight variation of the film thickness.

on the various dielectric substrates and analysis of the magnetooptical parameters of the produced structures as well as to comprehensive investigation of a role of the substrate and separate layers as well as the film/substrate interface in formation of the magnetooptical response of the nanostructures.

The study provides results of investigation of the magnetooptical Faraday and Kerr effects both in the BiYIG/r-Al_2O_3 nanostructures as well as in the r-Al_2O_3 single-crystal plates. The produced samples of the BiYIG films have the magnetooptical characteristics that are comparable in magnitude with the Faraday and Kerr effects in the BiYIG/GGG traditional structures. The study results are important for understanding the mechanisms of formation of the magnetooptical response in the nanoscale thin-film structures on the various substrates as well as for evaluating applicability of the sapphire substrates for manufacturing elements of the magnetooptical devices.

2. Experimental procedure and samples

The $BiY_2Fe_5O_{12}$ targets (a space group Iā3d (O_h)) for creating the films were produced by solid-phase synthesis. Figure 1, a shows diffraction patterns that are obtained by means of the X-ray spectrometer Dron-2M and confirm their single-phase nature and compliance of a chemical composition to the nominal one (the lattice constant is $a = 1.2444$ nm). The results of scanning electron microscopy (Tescan MIRA) with an energy-dispersive X-ray microanalyzer have shown (Figure 1, b) that in a microscale the target is quite loose and inhomogeneous in structure and composition: the scanning area has light and dark regions that are enriched with bismuth and yttrium, respectively. At the same time, iron is distributed evenly across the entire studied plane of the target. However, in an integral calculation (over the area) the chemical composition of the target coincides

with the nominal one within an error of the measurements.

The substrates were commercially available epi-polished (the average roughness is below 0.7 nm) r-Al_2O_3 single-crystal plates $[1\bar{1}02]$ of the sizes $10 \times 10\,mm^2$ and the thickness of 0.5 mm. The BiYIG/r-Al_2O_3 nanostructures with the nominal thicknesses of the layers $d = 5$, 11, 28, 44 and 54 nm were manufactured by magnetron sputtering with alternating current (13 MHz) at the substrate temperature $T = 200\,^{\circ}C$. Details of film synthesis are described in the studies [16,17].

In order to improve structural and magnetooptical perfection, the synthesized films were subjected to postgrowth annealing in a muffle furnace at $T = 650\,^{\circ}C$ in the argon atmosphere for 3 hours at the heating/cooling rate of 6 degrees per minute.

The produced film samples were tested by method of electron, optical and probe microscopy. It was shown by the electron microscopy that the films with $d = 5$ nm and 11 nm are characterized by a pronounced island structure. With increase of the layer thickness to $d \geq 28$ nm a portion of the islands is reduced and the films become more homogeneous (Figure 1, *c*). The magnetic-force images of the samples, which are obtained in the scanning probe microscope Solver Next (NT-MDT), visualize a domain microstructure with even surface distribution of typical sizes of the observed specific features (Figure 1, *d, f*). The results of electron microprobe analysis were used to record a small difference in the compositions of the films and the stoichiometric targets (not shown in the figure). For example, as compared to the initial target the films exhibit reduction of the Fe portion and an increase of the oxygen content. At the same time, cation and anion distribution is inhomogeneous across the film thickness, which seems to be caused by processes of diffusion of chemical elements at the interface boundaries. As a result, the measured composition of the BiYIG turned out to be close to $Bi_xY_{3-x}Fe_5O_{12}$, where $0.2 \leq x \leq 0.5$. These conclusions agree with the data of X-ray diffraction analysis and high-resolution transmission electron microscopy, which have been previously obtained for the films of a similar composition and thickness on the GGG substrates [17]. According to the results of optical profilometry (NewView 7300 ZygoLOT, Germany), the thickness of the obtained films is close to the nominal one, while average roughness of the film surfaces was $\sim 1-2$ nm (Figure 1, *e*). It makes it possible to neglect the contribution by diffusion reflection when measuring the magnetooptical effects in the visible spectral range.

In the ultra-fine magnetic films, an important role is played by a critical thickness (h) of the film-substrate interface — a relaxation layer, in which a high density of displacement dislocations is formed due to incompliance of the parameters of the crystal lattices of the film (a) and the substrate (b) [18,19]. These differences are characterized by an incompliance factor $f_c = (a - b)/a$ that shall be taken into account when creating and studying the thin-film nanostructures. As shown in the studies [13,16,20], for the BiYIG films on the garnet substrates, in case when the lattice parameters insignificantly differ ($f_c < 1\%$), within the framework of the Van der Merwe model the thickness of the relaxation layer, in which the displacement dislocations are completely removed in the film/substrate interface, is about $40-55$ nm. The sapphire single crystal has a crystal system Rc and is characterized by the lattice constants $b = 0.475$ nm and $c = 1.297$ nm [21]. Among the closest parameters is a distance between two adjacent planes in the r-Al_2O_3 substrate with the orientation $[1\bar{1}02]$ $a = 0.348$ nm [22]. For the BiYIG film, the analogous distance between the planes (321) is $a = 0.331$ nm.

Thus, in case of r-Al_2O_3 and $Bi_xY_2Fe_5O_{12}$ it is not possible to evaluate h by the Van der Merwe model both due to a difference of the symmetry of the crystal lattices of the film and the substrate and high differences of the parameters of the lattice cells. High mismatch of the lattice parameters presupposes formation of the film/substrate interface with a high density of the displacement dislocations, thereby preventing epitaxial growth of the singly-bound BiYIG films by the Van der Merwe model and contributes to formation of the island structures as per the Volmer-Weber type therein [19]. Formation of a damaged (magnetically dead and/or magnetically passive) layer within the film/substrate interface shall affect the magnetic and magnetooptical characteristics and, therefore, the Faraday and Kerr effects in the BiYIG/r-Al_2O_3 nanostructures.

We note that the Faraday effect is in a larger degree caused by volumetric properties of magnetics, so is the Kerr effect by surface characteristics of the structures and the separate layers. Therefore, it is desirable to measure both the effects when studying the magnetooptical properties of the films. In this study, the Faraday effect (FE) related to rotation of a polarization plane of linearly-polarized light transmitted through the sample was measured within the energy range from 1.5 to 4 eV in the constant magnetic field of up to $H = 10$ kOe in an original installation based on the monochromator MDR-12. It included a single-beam measurement procedure with the angle between the polarizer and the analyzer $\alpha = 45^{\circ}$ [23]. The polar Kerr effect (PKE) related to rotation of the polarization plane of linearly polarized light reflected from a surface of the normally magnetized sample was measured within the spectral range from 1.5 to 4 eV in an original installation based on the monochromator MDR-4. We used a single-beam dynamic method of PKE measurements for s-polarization light at the angle between the polarizer and the analyzer $\alpha = 45^{\circ}$ in the fields of up to $H = 12$ kOe that were modulated with the frequency of 2 Hz. Reflected light ellipticity was not determined due to measurement procedure restrictions. The measurement error was -5%. All the measurements were performed at the room temperature.

3. Magnetooptical characteristics of the r-Al_2O_3 substrate

When studying Faraday rotation in the low-magnetic media (paramagnetics and diamagnetics), the Verdet constant $V = \mathrm{FE}/(H \cdot d)$ is used as a parameter that characterizes rotatability of the polarization plane of linearly polarized light by the material under effect of the magnetic field [23]. Figure 2 shows the spectra $V(\lambda)$ for the r-Al_2O_3 substrates. The r-Al_2O_3 is characterized by an almost zero-dispersion progress of the curve within the entire studies spectral interval. The r-Al_2O_3 substrate has the least value of the Verdet constant among the materials studied by us. The rotation value for it is $V \sim +0.03\,\mathrm{min}/(\mathrm{Oe} \cdot \mathrm{cm})$, i. e. it is comparable with the values for the diamagnetic glasses SiO_2, BaB and NaCaSi [9]. Since in the diamagnetic materials the Verdet constant is proportional to $\sim 1/\lambda^2$ and increases as approaching a resonance absorption maximum (λ_0), then in case of r-Al_2O_3 according to the band gap width $E_g \sim 8.8\,\mathrm{eV}$ [24] the maximum of $V(\lambda)$ shall be attained when $\lambda_0 \sim 137\,\mathrm{nm}$. A large distance of the studied spectral interval from λ_0 possibly explains observed weak dispersion of the Verdet constant in sapphire.

If observation of Faraday rotation requires transparent substrates with a high optical quality of both the surfaces, then for the Kerr effect, in order to minimize contributions by the various resonance and magnetooptical effects related to light reflection from a back side of the substrate, the measurements are usually carried out on the epi-polished substrate, whose back side is rough or diffuse-scattering. In this study, the PKE spectral dependences were studied both on the polished substrate and the substrate with the diffuse-scattering back side that was mechanically ground using diamond pastes. Figure 2 illustrates that in the rough-side substrate PKE within the spectral interval $300 < \lambda < 800\,\mathrm{nm}$ ($4.1 < E < 1.5\,\mathrm{eV}$) has a negative sign and a low value within the measurement error ($< 0.5\,\mathrm{min}$). A similar pattern is observed for the substrate epi-polished at both sides. In this case, the Kerr effect still has the value and the negative sign, but the spectrum originates positive surges within the wavelength interval $400 < \lambda < 600\,\mathrm{nm}$ (Figure 3). The Kerr effect gets the maximum values of about $-1.5\,\mathrm{min}$ within the range $E \geq 3.5\,\mathrm{eV}$ ($\lambda < 330\,\mathrm{nm}$), in which interband optical transitions appear for r-Al_2O_3 [25,26].

As shown in the studies [20,27], the high values of the Kerr effect in the GGG-type transparent substrates can significantly contribute to the magnetooptical properties of the nanoscale structures. However, the r-Al_2O_3 epi-polished substrate has low magnetooptical activity except for the short-wavelength range and does not noticeably affect the characteristics of the structures. We note that the negative sign and the low value of the Kerr effect in the short-wavelength spectral range are comparable with the value and the sign of magnetic reflection ($\sim -10^{-4}$) of s-polarized light for the r-Al_2O_3 crystal [26,28], which is related to the influence of the external magnetic field on

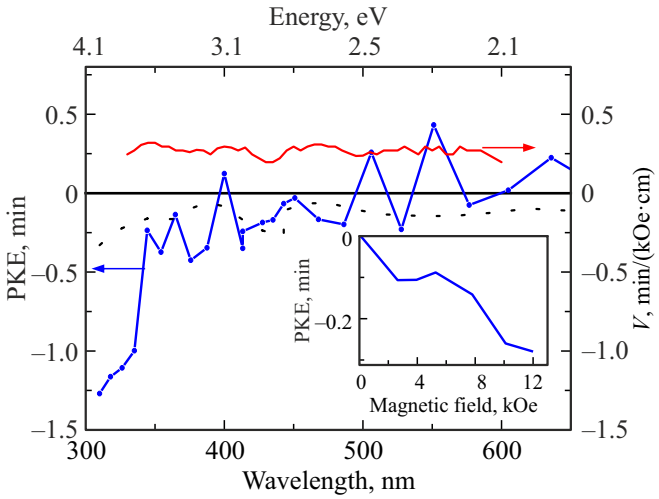

Figure 2. Spectra of the polar Kerr effect (PKE) for the substrate epi-polished at both sides (the solid lines) and the r-Al_2O_3 substrate with the diffuse-reflective back side (the dotted line) in the field of 7 kOe (the left scale) and the Verdet constant spectra (V) in the field of 4 kOe (the right scale). The insert has the PKE field dependence when $\lambda = 400\,\mathrm{nm}$ ($E = 3.1\,\mathrm{eV}$).

the optical properties of wide-band dielectrics of the Al_2O_3 type ($E_g \sim 8.8\,\mathrm{eV}$). The field dependences of the Kerr and Faraday effects (the insert of Figure 2) for the r-Al_2O_3 epi-polished substrate have the different sign and a diamagnetic-typical linear dependence without saturation in the magnetic fields of up to 10 kOe [7,9,11,29].

Thus, the values of Faraday and Kerr rotation in the r-Al_2O_3 transparent diamagnetic substrates in the visible spectral range are low and can any noticeably contribute to magnetooptical activity only within the wavelength range below 350 nm. Using the substrates with the diffuse-reflective (unpolished) back surface makes it possible to minimize the contribution by the substrate to the Kerr Effect for the BiYIG/r-Al_2O_3 nanostructure.

4. Magnetooptical characteristics of the BiYIG/r-Al_2O_3 nanostructures and the BiYIG films

4.1. Polar Kerr effect

The polar Kerr effect is an efficient tool for investigating and monitoring the magnetic characteristics of both the multilayer structures and the separate layers as well. Figure 3 show the spectra of the polar Kerr effect for the BiYIG/r-Al_2O_3 nanostructures as well as the respective BiYIG films of the thickness of $d \geq 28\,\mathrm{nm}$, which are obtained as a result of subtraction of the substrate spectrum. The high magnetooptical quality of the samples, the comparable values of the interface thicknesses in the nanostructures and the weak influence of the magnetooptical parameters of the substrate determine a

progress of the spectral curves and proximity of the PKE for the nanostructures and the films of the various thickness. However, the presence of the island growth structures in the films results in reduction of magnetization and a noticeable decrease of the rotation value (down to ~ 5 min) in the BiYIG/r-Al_2O_3 nanostructures as compared to the similar-composition nanostructures on the garnet substrates [16,20], in which it is about 15–25 min in the same conditions. For example, the PKE spectra that are typical for the BiYIG composition could be obtained only for the films of the thickness $d = 44$ and 54 nm. At the same time, the effect value is approximately in two times less than for the similar films on the GGG substrates [20].

The observed specific features of the PKE spectral curves when $\lambda_1 = 480$ nm ($E_1 \sim 2.6$ eV) and $\lambda_2 = 350$ nm ($E_2 \sim 3.1$ eV) can be related to the transitions $t_2(Fe^{3+}) \rightarrow t_{2g}(Fe^{2+})$ and $e_g(Fe^{3+}) \rightarrow e_g(Fe^{2+})$ in an octahedral sublattice [30–32]. However, for the hyperfine films of the thickness that is close to or below the critical one, presence of magnetic inhomogeneities in the film-substrate interface and in the film volume significantly affects a shape of the magnetooptical spectra. For example, for the film of the thickness of $d = 44$ nm the PKE spectrum has a shape that is typical for the composition $Bi_{0.5}Y_{2.5}Fe_5O_{12}$, while for the film with $d = 54$ nm it has a shape that is typical for the composition $Bi_{2.5}Y_{0.5}Fe_5O_{12}$ (a red shift of the peak in the spectrum). For the film thickness d$\leq$ 28 nm no reliable values of Kerr rotation could be obtained.

As shown in the study [20], the PKE spectra for the BiYIG/GGG high-quality magnetically-homogeneous films are close to each other and the effect reaches the maximum value ~ 20 min when $\lambda = 350$ nm ($E = 3.54$ eV). In our case, the small values of the Kerr effect spectral dependences can be related to magnetic inhomogeneity of the BiYIG films, thereby causing significant deterioration of the magnetic and magnetooptical properties of the BiYIG/r-Al_2O_3 nanostructures.

We should note the difference of the Kerr dependences obtained for the BiYIG/r-Al_2O_3 structures on the epi-polished and diffuse-reflective substrates (not shown in the figure), which is most pronounced within the short-wavelength range below 350 nm. It is obvious that it is related to complex contributions by the Faraday and Kerr effects with multiple transmission of light reflected from the back side of the substrate as well as to ellipticity of light [13,20,27].

As shown in the studies [16,20,27], the contribution by the substrates distorts the shape of the Kerr effect field dependences in the nanostructures. In this case, in the BiYIG/r-Al_2O_3 nanostructure low magnetooptical activity of the substrate slightly affects the Kerr effect field dependence (the insert of Figure 3, *a*). The Kerr effect field dependences exhibit a ferromagnetic-typical kink with attaining saturation in the fields $H_S \sim 1-2.5$ kOe (the insert of Figure 3, *b*), which is clearer after subtraction of the contribution by the substrate. Small differences in the value of H_S for the films with $d = 54$ and 44 nm are most likely caused by a

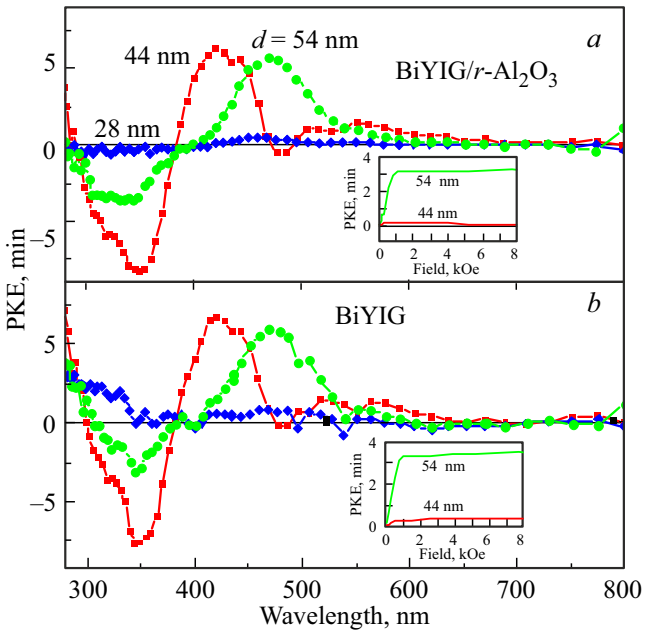

Figure 3. Spectra of the polar Kerr effect (PKE) for (*a*) the BiYIG/r-Al_2O_3 nanostructures and (*b*) the BiYIG films of the various thickness (shown in the figure) in the magnetic field $H = 4$ kOe. The film spectra are obtained after subtraction of the contribution by the substrates. The inserts include the PKE field dependences for the BiYIG/r-Al_2O_3 nanostructures (above) and the BiYIG films (below) at the wavelength $\lambda = 413$ nm ($E = 3$ eV).

different degree of magnetic inhomogeneity of the surface and the volume (possibly, by the different percent content of Bi and Y). This conclusion agrees with the data of the study [17]: with the film thickness below the critical one ($d < h$) diffusion of the elements at the interfaces results in formation of different-composition layers in the films. In turn, it results in formation of the magnetically dead and magnetically passive layers, reduction of magnetization and the Kerr effect and a change of the shape of the effect field dependences. The island structure of growth of the BiYIG films on r-Al_2O_3 just enhances the influence of these factors.

4.2. Faraday effect

Magnetic inhomogeneities in the BiYIG nanoscale films are also manifested in transmitted light in the Faraday effect spectral dependences. The island morphology of the film on the r-Al_2O_3 substrates results in reduction of magnetization and, consequently, reduction of Faraday rotation down to $\sim 10-20$ min within the wide spectral range from 320 to 650 nm (Figure 4, *a*). However, the shape of the spectral curves for the film $d = 54$ nm is still close to the FE spectra for the BiYIG films on GGG [20]. A negative part of the FE curve when $\lambda < 350$ nm is related to a charge-transfer transition from p-O states into a 3d-Fe state in the octahedral complexes [6,33]. The positive effect within the interval $350 < \lambda < 490$ nm is

related to the transitions of the type $t_2(Fe^{3+}) \rightarrow t_{2g}(Fe^{2+})$ and $e_g(Fe^{3+}) \rightarrow e_g(Fe^{2+})$. When $\lambda > 490$ nm, the FE spectrum is formed by electrodipole transitions from the 3d ground state into the hybridized Bi-O-Fe excited state in the octahedral [FeO] complexes [33–37].

Correlation of FE with the thickness of the BiYIG films is slightly traced from the obtained data. We should note that with the thicknesses below 28 nm the value of Faraday rotations drops to almost zero. Therefore, the results of measurements of the spectral and field FE dependences for the thinner films are not provided. Thus, if in the BiYIG thickness-similar films on GGG the maximum FE value reaches 1 degree [20], then in the BiYIG films on the r-Al_2O_3 substrate the effect decreases approximately in three times (≤ 20 min in the field $H \sim 7$ kOe) and can be reliably measured only for the films of the thickness $d = 44$ and 54 nm.

Both in the PKE case and for FE, rotation of the light polarization plane in the bulk substrates is additively manifested in the spectral and field dependences of the magnetooptical effects for the BiYIG/r-Al_2O_3 nanostructures (the insert of Figure 4, *a*). Thus, only after subtraction of the contribution by the substrates the field dependences of specific Faraday rotation F ($F = FE/d$) exhibit an inflection with attaining saturation both for magnetization as well as for PKE. At the same time, the maximum value of F is ~ 4 deg/μm in the fields $H > 2$ kOe for the wavelength of 413 nm (the insert in Figure 4, *b*). It is known that the typical values of specific rotation for the BiYIG crystals and the BiYIG thick films around the positive maximum are about 20−25 deg/μm (200000 deg/cm) in the fields $H_S > 2$ kOe [1,6–8,35,37–39]. The FE values obtained by us for the BiYIG/r-Al_2O_3 nanostructures is of the same order, which can indicate a satisfactory magnetooptical quality of the BiYIG produced films on the r-Al_2O_3 substrates.

In addition to the inflection, the curves $F(H)$ exhibit additional specific features (kinks), which are absent on the KE field dependences. Appearance of these specific features reflects specific features of the film state of BiYIG/r-Al_2O_3, which are related to deviation of a Bi/Y ion concentration ratio along the film thickness due to the specific features of the growth [17] and to the influence of the substrate. It is known that for the homogeneous films of a fixed composition the spectra and the values of $F(\lambda)$ shall be similar to each other and shall not depend on the type of the substrate and the structure thickness. This pattern is traced in the BiYIG/GGG(YAG) structures with the film thickness above the critical one ($d > 30$ nm) [16,20]. However, more pronounced magnetic inhomogeneity of the BiYIG films on r-Al_2O_3 results in higher distortion of the spectral and field dependences of the magnetooptical parameters, while in the films of the thickness $d < 28$ nm specific Faraday rotation generally tends to zero. The similar behavior of $F(\lambda)$ was observed in BiYIG on the garnet substrates only for the films of the thickness below 10 nm [16,20].

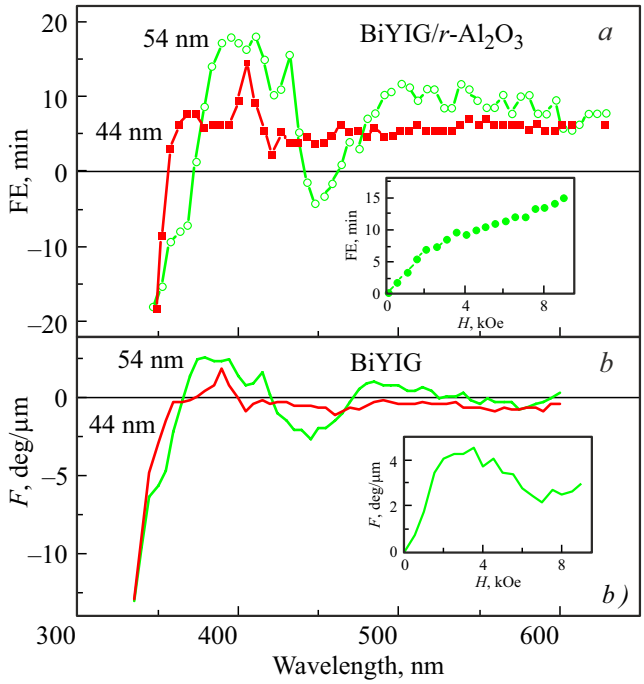

Figure 4. (*a*) Faraday effect (FE) spectral dependence for the BiYIG/r-Al_2O_3 nanostructures and (*b*) and the spectra of specific Faraday rotation (F) for the BiYIG films of the various thickness, which are obtained after subtraction of the contribution by the substrate, in the field $H = 7$ kOe. The inserts show the respective FE field dependences at the wavelength $\lambda = 413$ nm ($E = 3$ eV): (above) for the BiYIG/r-Al_2O_3 structure and specific Faraday rotation for the BiYIG film after subtraction of the contribution by the substrate (below).

Thus, the r-Al_2O_3 bulk transparent substrates have a minimum value of the magnetooptical effects with weak dispersion characteristics as compared to the garnet substrates. The magneto-optic Kerr and Faraday effects in the BiYIG/r-Al_2O_3 thin-film nanostructures attain the noticeable values in the visible spectral range in the magnetic fields above 2 kOe and are close in magnitude to the effects observed in the BiYIG thin-film structures on the garnet substrates.

5. Conclusion

We have considered the magneto-optic Faraday and Kerr effects in the thin-film magnetic nanostructures and the $Bi_xY_{3-x}Fe_5O_{12}$ films of the thickness 5, 11, 28, 44 and 54 nm, which were produced by magnetron sputtering on the r-Al_2O_3 diamagnetic dielectric substrates.

We have studied the specific features of the spectral and field characteristics of the Faraday effects and the polar Kerr effects in the plates of single-crystal sapphire with r-orientation. It is found that the magneto-optic effects for r-Al_2O_3 have weak dispersion in the spectral interval $300 < \lambda < 800$ nm: the polar Kerr effect varies

from -0.1 to -1.5 min, while the Verdet constant varies from $+0.01$ to $+0.03$ min/(Oe · cm). It is shown that for the $Bi_xY_{3-x}Fe_5O_{12}$ nanoscale films of the thickness above 44 nm specific Faraday rotation within the energy range 1.5–4.1 eV is higher than in the r-Al_2O_3 substrates and in the maximum reaches 40000 deg/cm in the magnetic field of 7 kOe, so does the Kerr effect — about 5 min in the field of 4 kOe. Thus, there is no need to take into account the contribution by the sapphire substrate when studying the magneto-optic effects in the $Bi_xY_{3-x}Fe_5O_{12}$/r-Al_2O_3 thin-film nanostructures.

The magnetic inhomogeneities in the $Bi_xY_{3-x}Fe_5O_{12}$ films are formed as a result of diffusion of the elements at the film/air and film/substrate interfaces, formation of pores and the high density of displacement dislocations in the interfaces [17]. In the $Bi_xY_{3-x}Fe_5O_{12}$/r-Al_2O_3 nanostructures with the island growth structure and the film thickness below the critical one, the magnetic inhomogeneities are enhanced. However, it results in insignificant (in 3–5 times) deterioration of their magnetooptical characteristics as compared to the similar-composition films on the garnet substrates.

The obtained values of the magnetooptical response in the $Bi_xY_{3-x}Fe_5O_{12}$/r-Al_2O_3 structures illustrate that they can be potentially applied both for fundamental research and for optimizing the procedures of synthesis of the magnetic nanostructures based on yttrium iron garnet and creating new functional elements of the optoelectronic devices on the r-Al_2O_3 substrates.

Funding

The study was conducted under the state assignment of the Ministry of Education of the Russian Federation for the Institute of Metal Physics, Ural Branch of the Russian Academy of Sciences. The films were formed by magnetron sputtering within the framework of RSF project No. 24-42-02008. The X-ray spectral and microscopic measurements of the samples were carried out in the Common Use Center of the Institute of Metal Physics, Ural Branch of the Russian Academy of Sciences.

Conflict of interest

The authors declare that they have no conflict of interest.

References

[1] A.K. Zvezdin, V.A. Kotov. Modern magnetooptics and magnetooptical materials. IOP Publishing, Bristol, Philadelphia, USA (1997), p. 381.
[2] B.J.H. Stadler, T. Mizumoto. IEEE Photonics Journal **6**, 0600215 (2014).
[3] S. Kharatian, H. Urey, M. Onbasli. Adv. Opt. Mat. **8**, 1901381 (2020).
[4] H. Alisafaee, M. Ghanaatshoar. Appl. Opt. **51**, *21*, 5144 (2012).
[5] A.V. Telegin, Yu.P. Sukhorukov. Magnetochemistry **8**, 173 (2022).
[6] V. Berzhansky, T. Mikhailova, A. Shaposhnikov, A. Prokopov, A. Karavainikov, V. Kotov, D. Balabanov, V. Burkov. Appl. Opt., **52**, *26*, 6599 (2013).
[7] S.M. Suturin, A.M. Korovin1, V.E. Bursian, L.V. Lutsev, V. Bourobina, N.L. Yakovlev, M. Montecchi, L. Pasquali, V. Ukleev. Phys. Rev. Mat. **2**, 104404 (2018).
[8] Yu.P. Sukhorukov, N.N. Loshkareva, E.A. Gan'shina, A.R. Kaul', O.Yu. Gorbenko, E.V. Mostovshchikova, A.V. Telegin, A.N. Vinogradov, I.K. Rodin. FTT **46**, *7*, 1203 (2004). (in Russian).
[9] J. Qiu, K. Hirao. J. Mat. Research **13**, *5*, 1358 (1998).
[10] E. Munin, J.A. Roversi, A.B. Villaverde. J. Phys. D: Appl. Phys. **25**, 1635 (1992).
[11] A.V. Starobor, D.S. Zheleznov, O.V. Palashov, E.A. Khazanov. J. Opt. Soc. Am. B **28**, *6*, 1409 (2011).
[12] A.K. Zvezdin, G.S. Krinchik, R.Z. Levitin, V.A. Lyskov. JETP Lett. **37**, *7*, 331 (1983).
[13] Yu.P. Sukhorukov, A.V. Telegin, I.D. Lobov, A.M. Korovin. Opt. and spektr. **132**, *7*, 733 (2024). (in Russian).
[14] N. Askarzadeh, H. Shokrollahi. Results in Chemistry **16**, 102390 (2025).
[15] N.V. Sharova, N.A. Popova, E.S. Lukin. Uspekhi v khimii i khimicheskoi tekhnologii **30**, *7*, 130 (2016). (in Russian).
[16] Yu.P. Sukhorukov, A.V. Telegin, I.D. Lobov, S.V. Naumov, S.S. Dubinin, K.A. Merencova, M.S. Artemyev, A.P. Nosov. J. Appl. Phys. **136**, 193905 (2024).
[17] I.A. Subbotin, E.M. Pashaev, A.O. Belyaeva, I.N. Trun'kin, S.S. Dubinin, K.A. Merentsova, M.S. Artem'ev, A.P. Nosov, A.L. Vasil'ev. Kristallografiya **70**, 529 (2025). (in Russian).
[18] J.H. Van der Merwe. Lattice mismatch and bond strength at the interface between oriented films and substrates. Pergamon Press, Oxford, London, New York, Paris (1964), p. 172.
[19] A. Fluri, C.W. Schneider, D. Pergolesi. In situ stress measurements of metal oxide thin films in book Metal oxide-based thin film structures. Elsevier, Amsterdam, Netherlands. (2017), p. 109–132.
[20] Yu.P. Sukhorukov, A.V. Telegin, I.D. Lobov, S.V. Naumov, S.S. Dubinin, K.A. Merencova, M.S. Artemyev, A.P. Nosov. J. Magn. Magn. Mater. **608**, 172415 (2024).
[21] E.M. Voronkova, B.I. Grechushnikov, G.I. Distler, I.P. Petrov. Opticheskie materialy dlya infrakrasnoi tekhniki. Nauka, M. (1965), s. 335. (in Russian).
[22] V.A. Lubarda, M.V. Lubarda. J. Am. Ceram. Soc. **106**, *3*, 2008 (2022).
[23] F.F. Sizov, Yu.I. Ukhanov. Magnetoopticheskie effekty Faradeya i Fogta v primenenii k poluprovodnikam. Naukova dumka, Kiev, Ukraina (1979), s. 182. (in Russian).
[24] M.E. Innocenzi, R.T. Swimm, M. Bass, R.H. French, A.B. Villaverde, M.R. Kokta. J. Appl. Phys. **67**, 7542 (1990).
[25] V.G. Kravets. Optics and Spectroscopy **98**, *3*, 405 (2005).
[26] B.B. Krichevtsov, A.M. Korovin, S.M. Suturin, A.V. Telegin, I.D. Lobov, N.S. Sokolov. Thin Solid Films **756**, 139346 (2022).
[27] S.M. Zanjania, M.C. Onbaşlí. J. Magn. Magn. Mater. **499**, 166108 (2020).
[28] W.Y. Lung, J.R. Chamberlain. Phys. Lett. **27A**, *6*, 365 (1968).
[29] S. Visnovsky, V. Prosser, R. Krishnan, V. Parizek, K. Nitsch, L. Svobodova. IEEE Trans. Magn. **17**, *6*, 3205 (1981).
[30] S. Visnovsky, R. Krishnan, V. Prosser. J. Appl. Phys. **49**, 2212 (1978).

[31] W.K. Li, G.Y. Guo. Phys. Rev. B **103**, *1*, 014439 (2021).
[32] F. Iori, A. Teurtrie, L. Bocher, E. Popova, N. Keller, O. Stéphan, A. Gloter. Phys. Rev. B **100**, 245150 (2019).
[33] S. Kahl, V. Popov, A.M. Grishin. J. Appl. Phys. **94**, *9*, 5688 (2003).
[34] E. Jesenska, T. Yoshida, K. Shinozaki, T. Ishibashi, L. Beran, M. Zahradnik, R. Antos, M. Kučera, M. Veis. Opt. Mat. Exp. **6**, *6*, 1986 (2016).
[35] M. Veis, E. Lišková, R. Antoš, Š. Višňovský, N. Kumar, D.S. Misra, N. Venkataramani, S. Prasad, R. Krishnan. Thin Solid Films **519**, 8041 (2011).
[36] T.G. Golovian, A.F. Konstantinova, E.A. Evdishchenko. Kristallografiya **66**, *3*, 341 (2021). (in Russian).
[37] K.M. Mukimov, B.Yu. Sokolov, U.V. Valiev. Phys. Stat. Sol. A **119**, 307 (1990).
[38] A. Hasanpoura, M. Mozaffaria, J. Amighiana, H. Richertd, A. Lorenzd, M. Lindnerd, P. Gornertd, H. Heegne. J. Magn. Magn. Mat. **317**, 41 (2007).
[39] M. Deb, E. Popova, A. Fouchet, N. Keller. J. Phys. D: Appl. Phys. **45**, 455001 (2012).

Translated by M.Shevelev